

## **A Study of the Equatorial Ionosphere Over Nairobi During Selected Magnetically Disturbed and Quiet Times for the Year 2009 Using Co-Located Instruments**

**Omondi George<sup>1</sup>, Ndinya Boniface<sup>1</sup>**

<sup>1</sup>Department of Physics and Materials Science,  
Maseno University, Maseno, Kenya

**Baki Paul<sup>2</sup>**

<sup>2</sup> Department of Technical and Applied Physics,  
Technical University of Kenya,  
Nairobi, Kenya

---

**Abstract:** Investigation of the behavior of the Equatorial Ionosphere over Nairobi-Kenya within the East Africa region is done using co-located instruments, that is, SCINDA-GPS system and a Magnetometer (MAGDAS). This was done for magnetically disturbed days, 22 and 23 July, 2009, as well as for quiet days before and after the geomagnetic disturbances. TEC depletions were observed and amplitude Scintillation indices plots were made and an attempt made to correlate these with modelled surface electric fields computed from magnetic field variations. The results show that most geoelectric field enhancements occurred between 0700 LT and 1300 LT mostly in the east-west component and in the post-midnight local time while scintillations and TEC enhancements and depletions occurred mostly between 0900 LT and 1100 LT during geomagnetic disturbances and between 1300 LT and 1400 LT during quiet times. This may be attributed to the development of the Equatorial Ionization Anomaly or an extension of the neutral wind dynamo driven by the E-region neutral wind and gravity waves generated by convection. Moreover, geoelectric field enhancements were accompanied by scintillations and TEC enhancements or depletions since pre-reversal enhancement in EXB drift controls the occurrence of scintillations.

---

### **1. INTRODUCTION**

Equatorial Ionization Anomaly (EIA) is a region of peak plasma density found at  $\pm 10^\circ$  to  $20^\circ$  magnetic latitudes at F-region altitudes. The behaviour of plasma understood by considering the motion of a charged particle in the presence of a magnetic field. The force acting on this particle is the Lorentz force given by:

$$m \frac{d\vec{v}}{dt} = q\vec{E} + q(\vec{v} \times \vec{B}) \quad (1.1)$$

where  $\vec{v}$  is the velocity,  $\vec{B}$  the external magnetic field,  $\vec{E}$  the electric field  $q$ , charge and  $m$  the mass of the particle. For steady motion of the charged particles, equation (1.1) reduces to

$$\vec{E} = -(\vec{v} \times \vec{B}) \quad (1.2)$$

Thus for a continuous motion of ionospheric plasma in the presence of the earth's magnetic field there must be an electric field perpendicular to both  $\vec{v}$  and  $\vec{B}$ . This condition is inferred from equation (1.2) after comparing it with the vector identity:

$$\hat{x} \times \hat{y} = -\hat{y} \times \hat{x} = \hat{z} \quad (1.3)$$

Solving for  $\vec{v}$  in equation (1.2) gives the expression

$$\vec{v} = \frac{\vec{E} \times \vec{B}}{|\vec{B}|^2} \quad (1.4)$$

Then the  $\vec{E} \times \vec{B}$  drift velocity is independent of charge (unidirectional at a time), hence the charges move in the same direction resulting in no net current. Equation (1.3) can be used to gain insight into the EIA and we investigate this in Nairobi, Kenya, which lies near the crest of the anomaly.

It is known that dynamic processes in the Sun affect the Earth's environment through geomagnetic disturbances. A geomagnetic disturbance (GMD) occurs when the magnetic field embedded in the solar wind is opposite that of the Earth (Barnes et al., 1999), that is, when the interplanetary magnetic field (IMF) is southward pointing. Energy is transferred from the solar wind by magnetic reconnection between the IMF and Earth's magnetic field (Gonzalez et al., 1994). Some geomagnetic storms, particularly larger ones, begin with the arrival of an interplanetary shock structure, called a *geomagnetic sudden impulse*. The shock front compresses the magnetosphere on the Sun side of Earth and is measured by magnetometers as a sudden discontinuous jump in amplitude of the horizontal field component. If the IMF associated with the arrival of a solar-terrestrial disturbance remains northward behind the shock then usually, there is no subsequent storm, and the shock stands alone as a *sudden impulse*. The consequence of the southward orientation of the IMF-Bz is the magnetic reconnection processes which permit the transportation of solar wind energy into the Earth's magnetosphere, thereby causing magnetic storms and the impulse is called a *sudden commencement*. The next (or sometimes first) appearance of the storm is called the main phase (growth phase) in which this principal component of the field decreases. Finally, in a recovery phase, the storm spends its greatest time gradually returning to an undisturbed level over as much as several days (Bernhardi et al., 2008).

Measurements of the strength of geomagnetic storms have been undertaken since 1840 using geomagnetic indices. The indices help to quantify the influence of solar disturbances on the Earth's magnetic field and differ in the time scale associated with their determination, for example, hourly, 3-hourly and daily. The Kp-index is an approximately logarithmic measure of magnetic disturbances and consists of ten values, Kp-0(no activity) through Kp-9 (major storm). It is related to the *peak-to-peak* fluctuations of the horizontal magnetic field component observed on a magnetometer during a three-hour interval relative to a quiet day. The vertical component (Z) is excluded from the K-index because it is more affected by underground-induced effects and by field sources farther from the station (Mayaud, 1980). The disturbance storm time (Dst) index estimates the globally averaged change of the horizontal component of the Earth's magnetic field at the magnetic equator based on measurements from a few magnetometer stations. A geomagnetic storm conditions prevail whenever Dst values are less than  $-50nT$  and an actual global geomagnetic storm is an event with values between  $-50nT$  and  $-100nT$  that lasts for at least four consecutive hours (Foster and Jakowski, 2000). Other indices include the A-index, Auroral electrojet (AE), Auroral Upper envelope (AU), Auroral Lower envelope (AL) and Equatorial Electrojet (EE).

The effects of geomagnetic activity are observed on technological systems, power grids, pipelines, telegraph lines and referred to as geomagnetically induced currents (GIC) (Boteler et al., 1998, Pirjola, 2000).

The physical principle of the flow of GIC in a technological system can be easily understood based on Faraday's law of induction that deduces the existence of a geoelectric field during a temporal variation of the geomagnetic field. The geoelectric field induces GIC in the conductor. Then GIC in a given conductor system is closely related to the time derivative of the magnetic field measured at a nearby location (Viljanen et al, 2001). This provides a pragmatic tool for deriving statistical predictions of the occurrence of GICs using the measured geomagnetic field. Together with simplified models of the ground conductivity, a plane wave assumption results in easy calculations of the geoelectric field (Pirjola, 2002). Studies by Rao et al., (2009), have established that, in the longitude sectors where the main phase of the geomagnetic storm occurs during the local sunset hours, there is a greater probability of the storm induced electric fields to contribute to the increase in the eastward electric fields enhancing the post sunset  $E \times B$  vertical drifts at the equator. These vertical drifts may result in conditions whereby ionospheric plasma densities and electric fields develop irregular structures with scale lengths from hundreds of kilometers down to sub-meter sizes, a condition known as equatorial spread F (ESF). These

turbulent ionospheric conditions were given a name “spread-F” primarily because of the way they affect the F layer trace in ionograms, by producing spreading in the echo range and frequency.

Plasma depletions, which are a manifestation of plasma bubbles, are the irregularities of the largest scale sizes (up to a few hundred km) that are associated with the ESF (Datta-Barua et al., 2010, Valladres et al C.E, 2004) These plasma irregularities in the F region of the equatorial ionosphere manifest as diffused echoes on the ionograms and generally occur during nighttime and are observed to be aligned to the Earth’s magnetic field (Tsunoda, 1980) The presence of plasma irregularities within these depletions disrupts communications and navigation systems by scattering radio wave signals that pass through them, a phenomenon known as ionospheric scintillation. The occurrence of these scintillations as satellite signals pass through the ionosphere is a clear indication of the fluctuations in the total electron content (TEC) of the ionosphere. From a recent study (D’ujanga et al., 2012). discussed the effects of the geomagnetic storm of the 24–25 October 2011 on the ionospheric TEC at the two East African stations located at Makerere University, Uganda (Lat: 0.3° N; Lon: 32.5° E) and at the University of Nairobi, Kenya (Lat: 1.3° S; Lon: 36.8° E). They noted a significant decrease in the diurnal variation of TEC and a deeper TEC depletion at both stations during the period of the storm. These effects during the storm were attributed to the uplift of the ionospheric plasma, which was then transported away from this region by diffusion along magnetic field lines. In another study, Falayi and Rabiou (Falayi and Rabiou, 2012) have investigated the interrelationship between the monthly means of time derivatives of horizontal geomagnetic field (dH/dt), sunspot number (Rz) and aa index for 232 substorms (-90nT-1800nT) between the years 1990 and 2009. They noted that the time derivative of the horizontal component of geomagnetic field (dH/dt) exhibited high positive correlation with sunspot number (0.86) and aa index (0.8998).

In the present study, we investigate the behaviour of the equatorial ionosphere over Nairobi using co-located instruments (SCINDA-GPS) and a magnetometer (MAGDAS) during magnetically disturbed and quiet times in the solar minimum year 2009. We establish a relationship between the electric field variations which are proportional to the time derivative of the horizontal component of the geomagnetic field (dH/dt), the Scintillations index (S<sub>4</sub> index) and Total Electron Content (TEC) for selected geomagnetically disturbed days and quiet days of July 2009. The results are then discussed and conclusions drawn.

## **2. DATA AND METHODS OF ANALYSIS**

The data used in this research are July 2009 H and D components of the geomagnetic field obtained from the Nairobi MAGDAS station and the ionospheric scintillations and total electron content were measured using NovAtel GSV400B GPS SCINDA at the university of Nairobi (Lat: 1.3° S; Lon: 36.8° E), for the year 2009. We consider the geomagnetically disturbed days 22<sup>nd</sup> July, 2009 when the Kp-index was 5 and 23<sup>rd</sup> July, 2009 that was the recovery phase of the storm.

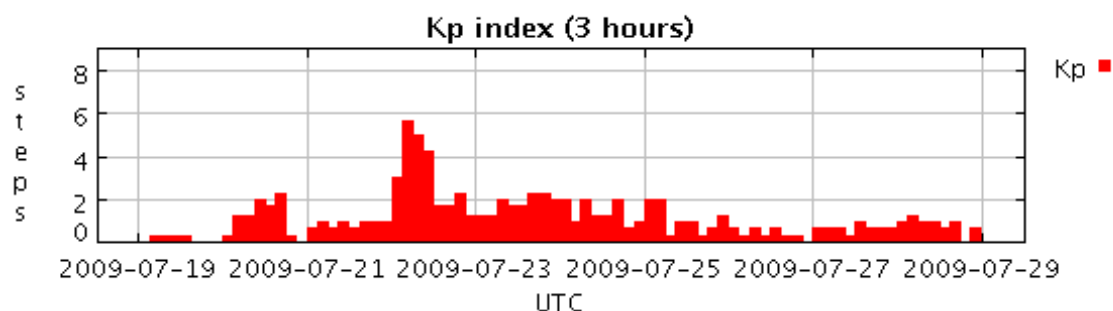


**Fig 1.** Kp indices between 19 July, 2009 to 28 July, 2009  
(<http://spidr.ngdc.noaa.gov/spidr/save.do?task=print>)

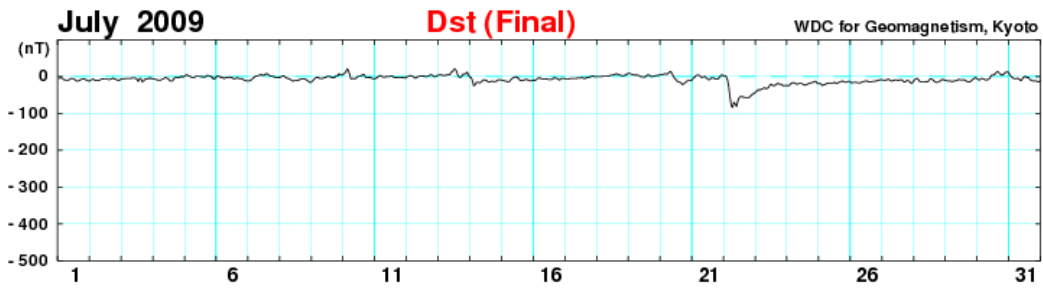


Fig 2. Dst Index for July, 2009 (wdc.kugi.kyoto-u.ac.jp/dst\_final/200907/index.html).

We also consider two quiet days before and after 22<sup>nd</sup> July, 2009

### 2.1. Computation of the Geoelectric Field

The geoelectric field which is a driver of GICs has a direct mathematical relationship with the time derivative of the geomagnetic field in accordance with Faraday’s law of electromagnetic induction. The magnetic data of Nairobi MAGDAS station availed the horizontal intensity,  $H$  (n T), declination,  $D$  (radians) and the vertical component,  $Z$  (n T) of the geomagnetic field. The northward and eastward components of the geomagnetic field respectively, were then obtained by use of the relations:

$$B_x = H \cos D \tag{2.1}$$

$$B_y = H \sin D \tag{2.2}$$

The time derivative of the northward component of the geomagnetic field on was calculated using the relation:

$$\frac{dB_{x,y}}{dt} = \frac{B_{x,y} \text{ t min} - B_{x,y} \text{ t-1 min}}{1 \text{ min}} \tag{2.3}$$

where  $t$  and  $t-1$  denote instances of time while min denotes minutes.

The geoelectric field was determined using the plane wave model, (Gaunt and Coetzee, 2007) which assumes that the primary field is a vertically propagating plane wave and the Earth’s conductivity is uniform. This method has been proved to be adequate because the calculated values correlated well with actual measured values (Gaunt and Coetzee, 2007). Assuming that the magnetic and electric fields are mutually orthogonal at the equatorial latitudes, the geoelectric field components  $E_{x,y}$  can be calculated as:

$$E_{x,y} = \pm \frac{1}{\sqrt{\pi\sigma\mu_0}} \int_{-\infty}^t \frac{1}{t-u} \frac{dB_{y,x}(u)}{dt} du \tag{2.4}$$

where  $\mu$  is the permeability of free space and  $\sigma$  is the ground conductivity. The time derivatives of the geomagnetic field are practically realized as discrete sequence of values hence transforming the infinite interval into a finite interval and applying the summation by parts, the discrete analogue to integration by parts, (Bernhardi et al. 2008) equation (2.4) takes the form

$$E(T_N) = \frac{2}{\sqrt{\pi\sigma\Delta\mu_0}} (R_{N-1} - R_N - \sqrt{M} b_{N-M}) \tag{2.5}$$

where  $\Delta$  is the sampling interval,  $N$  is the sample number and  $M$  is the number of previous time steps considered and

$$R_N = \sum_{n=N-M+1}^N b_n \sqrt{N-n+1} \tag{2.6}$$

where  $b_n = B_n - B_{n-1}$  in which  $B$  is the magnetic field component.

For the geomagnetic disturbed day, 22 July 2009, the H and D component of the magnetic data were substituted to equation (2.1) to obtain the magnetic field components. The magnetic field components were used in equation (2.5) to obtain the geoelectric field. A graph of northward and eastward components of the geoelectric field against time for day was plotted and the results shown in figures 3 (i) and 3 (ii) respectively. Similarly for days 19, 21, 23, and 28 July 2009, the graph of geoelectric field against time was plotted and the results shown in figures 4 (i) and 4 (ii), 5 (i) and 5 (ii), 6 (i) and 6 (ii) and 7 (i) and 7(ii), respectively.

## 2.2. Scintillation index and Total Electron Content

The processing of the S4 index and relative TEC obtained from Nairobi SCINDA station was performed using GPS TEC analysis software developed by Seemala and Valladres (2008) of the Institute of Scientific Research, Boston College, USA. The software includes an algorithm for the estimation or downloading of the satellite and receiver biases. The biases free TEC (Vertical TEC) is written in ASCII format together with other parameters which define the position of the satellite such as the time, elevation angle, azimuth angle and latitude of the Ionospheric Pierce Points (IPP). The output of the analysis includes TEC 24 hours images for all pseudorandom numbers (PRNs), PRN images and TEC plots for individual PRNs. The resulting TEC plots were analyzed to establish EPBs and associated GPS scintillations during the selected days. The scintillation index,  $S_4$ , and TEC data used in this study was that for PRN08 satellite. This is due to the fact that it had an elevation mask angle greater than  $30^\circ$  hence avoiding the effects of low elevation mask angles such as tropospheric, water vapour scattering and multipath effects. At low elevation angles high  $S_4$  index (greater than 0.6) values are observed because the amplitude scintillation depends on the electron density deviations and on the thickness of the irregularity layer, both of which increase apparently at low elevation angles, causing stronger scintillations and high  $S_4$  index values due to multipath effects (D’ujanga et al. 2012).

The graphs of  $S_4$  index and VTEC against time for 22<sup>nd</sup> July, 2009 was drawn and the result is as shown in figure 3 (iii). The same procedure was repeated for the other four days considered and the results are shown in figures 4(iii), 5 (iii), 6 (iii) and 7 (iii) respectively.

## 3. RESULTS AND DISCUSSION

### 3.1. Geomagnetically Disturbed Days

The results for the geoelectric field variations,  $S_4$  and VTEC are shown in figures 3 and 4.

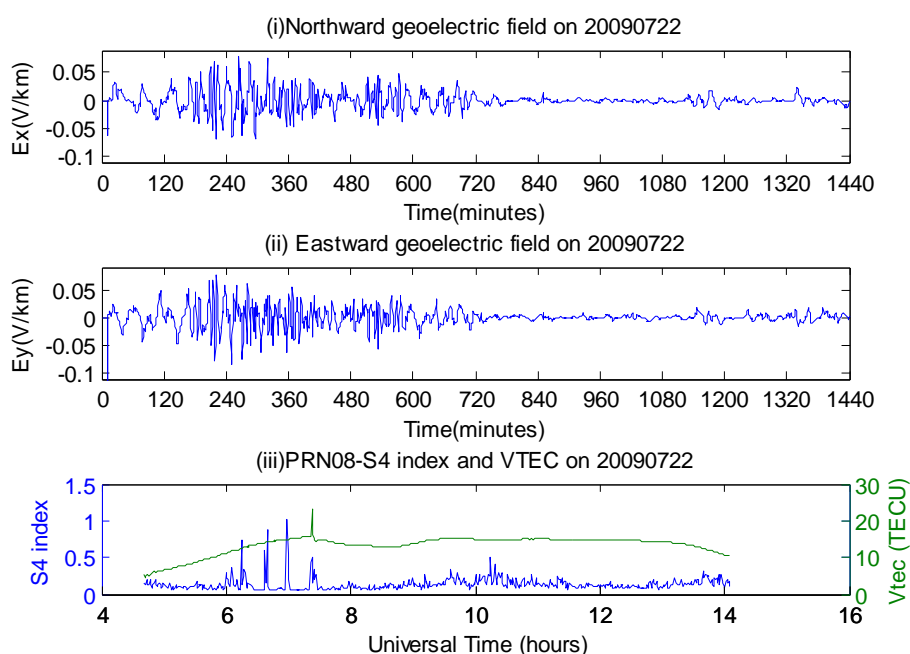


**Fig 3.** Geoelectric field variation,  $S_4$  and VTEC on 22 July, 2009

Figure 3 indicates shallow depletion in the TEC between 0800-0900 UT (1100h-1200h LT) and scintillations between 09.00 LT and 10.00 LT. A reduction in the scintillation index after 11.00 LT resulted in the depletion in the TEC values as well.

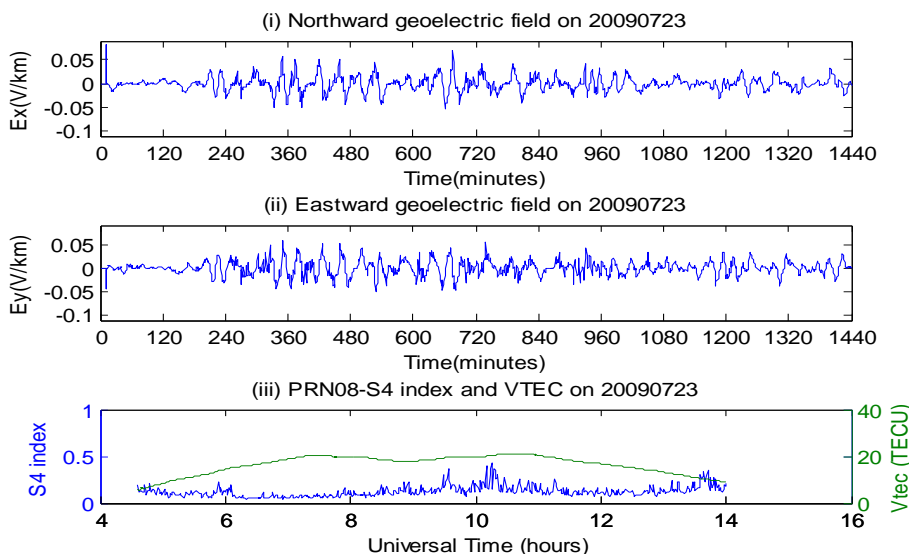


Fig 4. Geoelectric field variation,  $S_4$  and VTEC on 23 July, 2009

On 23 July, 2009 it is observed that the scintillation index values increased between 11.00 LT and 14.00 LT. At the same time, there were depletions in the TEC values. At 14.00 UT, there was a rise in the scintillation index but a depletion in the TEC values.

Most enhancements in the electric field occurred between the period 240 minutes and 600 minutes. That is, between 0700 LT and 13.00 LT. Another period when noticeable enhancements in the electric field were observed was between 960 minutes and 1080 minutes. That is, between 1900LT and 21.00 LT.

### 3.2. Geomagnetically Quiet Days

The results for the geoelectric field variations,  $S_4$  and VTEC for the geomagnetically quiet days are shown in figures 5 to 7.

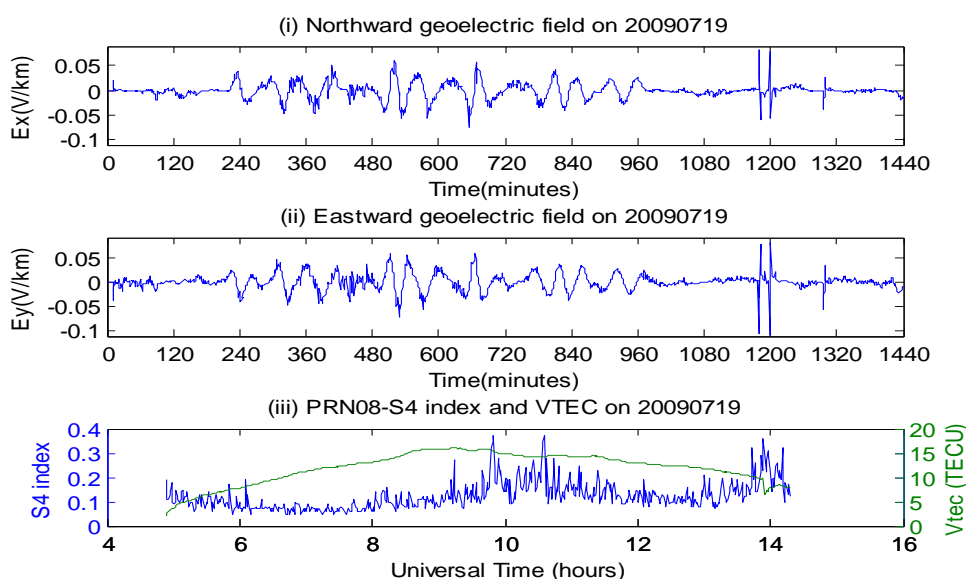
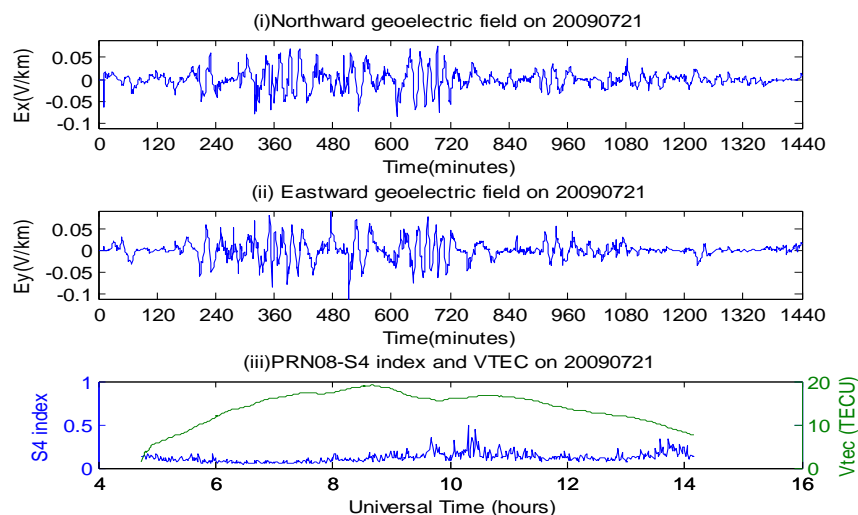
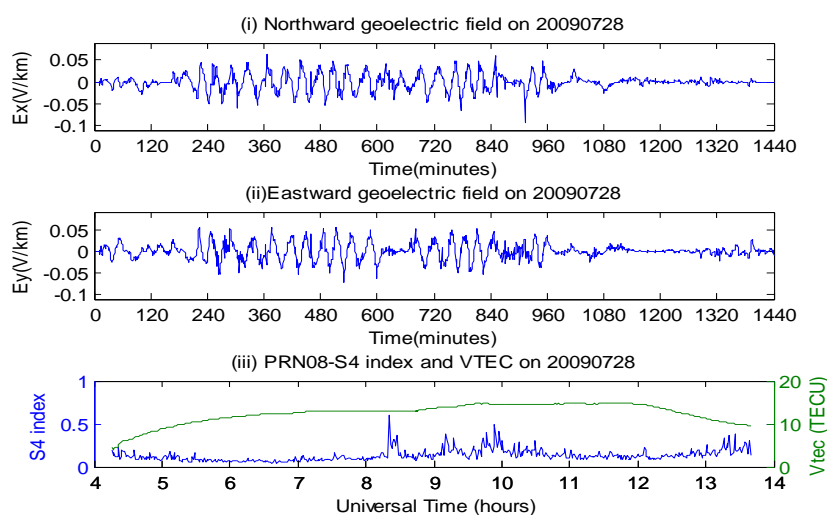


Fig 5. Geoelectric field variation,  $S_4$  and VTEC on 19 July, 2009



**Fig 6.** Geoelectric field variation,  $S_4$  and VTEC on 21 July, 2009



**Fig 7.** Geoelectric field variation,  $S_4$  and VTEC on 28 July, 2009

During the quiet days shown figures 5,6 and 7 most of the enhancements in the electric field were noticed within the interval of 240 minutes and 600 minutes (0700 LT-1300 LT). It is observed that most of the scintillations increased between 08.00 UT and 11.00 UT. Moreover, during these times, there were TEC depletions as expected. Scintillation index again increases at about 14.00 UT accompanied with depletion in the TEC. However, by extrapolation there are also scintillations during the evenings ( post sunset periods)

It is important to note that all the plots of the electric fields above begin at 00.00 UT (03.00 LT in Nairobi). From the graphs of geoelectric field variations, it is observed that there are anomalous enhancements in the surface electric field in the post-sunset and post-midnight local time during both disturbed and quiet times. The enhancements occurred mostly in the eastward component and in some cases in the northward component as well.

The enhancement in the eastward electric field during postmidnight local time is attributed to neutral wind dynamo driven by E- region neutral-wind, gravity waves generated by convection (Yizengaw et al., 2009). Another possible source of night time electric fields is the F-region dynamo triggered by thermospheric neutral winds. In this case, the positive gradient of the F-region zonal neutral wind (increasing eastward with time) would result in an eastward electric field which then produces vertically upward drift velocity and causes the formation of EIA in the postmidnight sector. Dispersion of atmospheric dust particles into the atmosphere and the associated friction can result in acquisition of an electric charge by the particles (Yizengaw et al., 2013 and references there in). The charged dust particles are then transported to high altitudes

through wind gusts that raise local dust into the upper atmosphere especially over the Sahara desert in Africa. In addition, it is known that neutral winds in Kenya flow from West to east in the evening (Mukabana and Pielke, 1996) and that this could lead to production of electric fields enhancement.

In the study done by Shankar (2007), it was determined that EIA develops gradually in the day, peaking between 1100 hours LT to 1400 hours LT and falls in the night time. In addition, signatures of the pre-reversal drift enhancement due to enhanced post sunset F-region vertical drifts appear between 1900 to 2100 LT. This may be considered to account for the above results.

#### 4. CONCLUSIONS

Wang et al (2008) established short-term correlation between TEC and geomagnetic activity specifically the Dst index. As the geomagnetic activity increases, the correlations also increase rapidly from morning to afternoon. These correlations exist even during quiet times. The results of the present study also show that the geoelectric fields, scintillation and TEC enhancements are high during geomagnetic storms but a little lower during quiet times. This is attributable to the fact that during geomagnetic disturbances a lot of particles in form of CMEs are ejected from the sun into the solar-terrestrial atmosphere enhancing electric fields, ions and scintillations in the upper atmosphere. However, this is not true for all the days since the storm on 22 July, 2009 was shortlived.

The results also show that most scintillations were accompanied by enhancements in the geoelectric fields. This may be as a result of the time lag between the occurrence of a geomagnetic disturbance and the impact of the disturbance on the surface of the Earth. This is because the CMEs and solar wind from the sun are ejected at various speeds depending on the solar activity.

It is important to note also that scintillations and TEC depletions and enhancements occur both during geomagnetic disturbances and quiet times especially within the equatorial sector.

There is generally positive correlation between the shallow depletions (about a depth of 2 TECU) and electric field enhancements as shown in figure 3, figure 5 and figure 6. Not all TEC depletions were accompanied any observable variations in the geoelectric fields. Hence the occurrence of a TEC depletion may not necessarily translate into enhancement in the electric field.

In general the present study has shown a positive correlation between TEC and scintillation with the geoelectric field.

#### ACKNOWLEDGEMENT

We wish to acknowledge Departments Of Physics and Geology for availing ground resistivity data and allowing us to use all the data. We also sincerely appreciate the Boston University for SCINDA-GPS, MAGDAS team in collaboration with Kyushu University, Japan for installing the magnetometer in Nairobi, Kenya that helped in data acquisition. I also thank Maseno University for financing my research.

#### REFERENCES

- Barnes P.R, D.T Rizy and B.W. McConnell, Electric Utility Industry Experience with geomagnetic disturbances, Oak Ridge National Laboratory Power Systems Technology Program, 1999.
- Boteler D. H., R. J. Pijola and H. Nevanlinna, The effects of geomagnetic disturbances on electrical systems at the earth's surface, *Adv. Space Res.* Vol. 22, No. 1, pp. 11-21, 1998.
- Bernhardi E.H. et al., Improved calculation of geomagnetically induced currents in power networks in low-latitude regions, *PSSC Proceedings* pg.677, 2008.
- Datta-Barua, S., Doherty, P. H., Delay, S. H., Dehel, T., and Klobuchar, J. A., Ionospheric Scintillation Effects on Single and Dual Frequency GPS Positioning, *Proceedings of the 16th International Technical Meeting of the Satellite Division of The Institute of Navigation (ION GPS/GNSS 2003)*, Portland, OR September 2003, 336–346, 2010

**A Study of the Equatorial Ionosphere Over Nairobi During Selected Magnetically Disturbed and Quiet Times for the Year 2009 Using Co-Located Instruments**

- D'ujanga F.M., P. Baki, J.O. Olwendo and B.F. Twinamasiko, Total electron content of the ionosphere at two stations in East Africa during the 24–25 October 2011 geomagnetic storm, *Advances in Space Research* 51, 712-721, 2013, <http://dx.doi.org/10.1016/j.asr.2012.09.040>
- Falayi E. O. and A. B. Rabi, Dependence of Time Derivative of Horizontal Geomagnetic Field on Sunspot Number and aa Index, *Frontiers in Science* 2012, 2(1): 1-5
- Forster M. and N. Jakowski Geomagnetic effects on the topside ionosphere and plasmasphere: a compact tutorial. *Surv. Geophys.* 21, 47–87, 2000
- Gaunt C.T and G. Coetzee , Transformer failures in regions incorrectly considered to have low GIC-risk, 2007 <http://www.labplan.ufsc.br/congressos/powetec>.
- Gonzalez W., J. Joselyn, Y. Karmide, H. Kroehl, G. Rostoker, et al., What is a Geomagnetic Storm?, *Journal of Geophysical Research*, Vol. 99, No. A4, Pg 5771-5792, Apr 1, 1994
- Mayaud P., Derivation, Meaning, and Use of Geomagnetic Indices, American Geophysical Union, 1980
- Mukabana J.R and Pielke R.A, Investigating the Influence Of Synoptic-Scale Monsoonal Winds and Mesoscale Circulations on Diurnal Weather Patterns over Kenya using Numerical Model, American Meteorological Society, *Monthly Weather Review* vol. 124, (1996)
- Rao P.V.S.R., S.G. Krishna, J.V. Prasad, and, K. Niranjana ,Geomagnetic storm effects on GPS based navigation. *Ann. Geophys.* 27, 2101–2110, 2009
- Risto Pirjola, Geomagnetically Induced Currents during Magnetic Storms, *IEEE Transactions On Plasma Science*, Vol. 28, No. 6, December 2000 pg. 1867.
- Risto Pirjola, Review on the calculation of surface electric and magnetic fields and of geomagnetically induced currents in ground-based technological systems, *Surveys in Geophysics* 23: 71-90, Netherlands ,2002
- Shankar J., Analysis of the day side equatorial anomaly, Msc. thesis, Utah State University, Logan, Utah ,2007.
- Shin Soon JA, Analysis Of Total Electron Content (TEC) Variations in the Low- and Middle-Latitude Ionosphere, All [http:// digitalcommons.usu.edu/etd/403](http://digitalcommons.usu.edu/etd/403) ,2009.
- Tsunoda, R.T. Magnetic-field-aligned characteristics of plasma bubbles in the nighttime equatorial ionosphere. *J. Atmos. Terr. Phys.* 42, 743–752, 1980.
- Valladares C.E., J. Villalobos, , R. Sheehan M.P. Hagan Latitudinal extensions of low-latitude scintillations measured with a network of GPS receivers. *Ann. Geophys.* 22, 3155–3175, 2004.
- Viljanen, A., H. Nevanlinna, K. Pajunpaa and A. Pulkkinen, Time derivative of the horizontal geomagnetic field as an activity indicator, *Ann. Geophys.*, 19, 1107–1118, 2001.
- Wang X.Q., R.S Eastes and C.E.Valladares, Short-term relationship of total electron content with geomagnetic activity in equatorial regions, *J.Geophys.Res.*,113, A11308, doi:10.1029/2007JA012960 ,2008.
- Yizengaw E. et al., Strong postmidnight equatorial ionospheric anomaly observations during magnetically quiet periods, *J. Geophys. Res.*114, A12308, doi:10.1029/2009 JA014603, 2009.
- Yizengaw, E.,J. Retterer, E. E. Pacheco, P. Roddy, K. Groves, R. Caton, and P. Baki ,Postmidnight bubbles and scintillations in the quiet-time June solstice, *Geophys. Res. Lett.*, 40, doi:10.1002/ 2013GL058307 (2013).